Semiconducting, defect-free polymorph of borophene: Peierls distortion in two-dimensions

S. İpek,[1] M. E. Kilic,[2] A. Mogulkoc,[3] S. Cahangirov,[2] and E. Durgun[2,*]

[1]*Department of Engineering Physics, Istanbul Medeniyet University, Istanbul 34700, Turkey*

[2]*UNAM - National Nanotechnology Research Center and Institute of Materials Science and Nanotechnology, Bilkent University, Ankara 06800, Turkey*

[3]*Department of Physics, Faculty of Sciences, Ankara University, 06100, Tandogan, Ankara, Turkey*

(Dated: November 25, 2018)

Abstract

In contrast to the well-defined lattices of various two-dimensional (2D) systems, the atomic structure of borophene is sensitive to growth conditions and type of the substrate which results in rich polymorphism. By employing *ab initio* methods, we reveal a new, thermodynamically stable borophene polymorph without vacancies which is a semiconductor unlike the other known boron sheets, in the form of an asymmetric centered-washboard structure. Our results indicate that asymmetric distortion is induced due to Peierls instability which transforms symmetric metallic system into a semiconductor. We also show that applying uniaxial or biaxial strain gradually lowers the obtained band gap and symmetric configuration is restored following the closure of the band gap. Furthermore, while the Poisson's ratio is calculated to be high and positive in semiconducting regime, it switches to negative once the metallicity is retrieved. The realization of semiconducting borophene polymorphs without defects and tunability of its electronic and mechanical response can extend the usage of boron sheets in variety of nanoelectronic applications.

Boron has a short covalent radius, owns delocalized electrons, and can adopt sp^2 hybridization likewise carbon, which lead to formation of numerous low-dimensional structures, including nanotubes[1], fullerenes[2,3], and clusters[4]. Following the realization of quasi-planar small boron clusters[5,6], various two-dimensional (2D) boron sheets, namely borophene[5,7] with similar cohesive energies are also predicted. The vacancies[8] and/or out-of-plane distortions[9] have been shown to enhance the stability of these structures. In parallel with theoretical envisions closed-packed, triangular buckled[10] and planar triangular polymorph of borophene with different vacancy patterns[11] are grown on Ag(111) substrate. Very recently, the coexistence of two distinct polymorphs of borophene with line defects have been revealed experimentally on Ag(111) substrate[12].

Depending on its structure and geometry borophene posses novel properties which differ significantly from bulk counterparts. For instance, while bulk structures of boron are semiconductor, borophene polymorphs[13] are metallic[10–12]. Recently, two phases of borophene (β_{12} and χ_3 sheets) are predicted to have phonon-mediated superconductivity with considerably high critical temperature[14]. β_{12}-borophene also hosts gapless Dirac cones mainly contributed by the p_z orbital of boron[15]. This prediction is further confirmed experimentally based on angle-resolved photoemission spectroscopy (ARPES) results[15]. Buckled phase of borophene (δ_6-borophene) has corrugated rows of atoms in one lattice direction, resulting in strong anisotropy in electronic[10,16], mechanical[10,17], thermal[18,19], and optical properties.[16,20] Owing to peculiar properties of borophene allotropes, these systems are promising candidates to be used in various technological applications including flexible optically transparent electrode devices[21,22], electrocatalyst for the hydrogen evolution reactions[23], thermal management applications for the efficient heat transport[24], and electronic junctions based on self-assembled heterostructures[25].

In contrast to the well-defined lattices of various 2D systems, borophene can exhibit variety of polymorphs resulting from both intrinsic factors such as multi-center bonding scheme of boron atoms and extrinsic factors including substrate type and growth conditions[26]. Accordingly, different polymorphs of borophene with similar cohesive energies[7] but with distinct properties can be obtained. Motivated by the recent advances in borophene, in this Rapid Communication we explore rare borophene polymorphs without vacancies/defects, and show that thermodynamically stable, asymmetric centered-washboard structure which is similar to the geometry of monolayer black phosphorus can be obtained. Following the analysis of

structural properties, we reveal the origin of asymmetric distortion (Peierls instability) which transforms metallic system into a semiconductor by opening a gap in the electronic band structure. We also examine the electronic and mechanical response of the system to applied uniaxial or biaxial strain and obtain semiconductor to metal phase transition together with a positive to negative Poisson's ratio alteration.

We carried out first-principles calculations based on spin-polarized density functional theory (DFT)[27,28] implemented in Vienna *ab initio* simulation package (VASP)[29]. The projector-augmented-wave (PAW) potentials[30] with kinetic energy cutoff of 420 eV for the plane-wave basis set was used. The generalized gradient approximation (GGA) within Perdew, Burke, and Ernzerhof (PBE) scheme[31] was utilized to describe the exchange-correlation potential. The electronic band structure calculations were also calculated with hybrid functionals (HSE06)[32] to correct the underestimated band gap values. All atomic positions and lattice constants are optimized using the conjugate gradient method without any constraints by setting convergence criteria on the total energy and force to 10^{-5} eV and 10^{-2} eV/Å, respectively. A Γ-centered $20 \times 16 \times 1$ k-point mesh is used for the Brillouin zone integrations of the primitive unit cell and then scaled accordingly with the cell size. A super cell geometry with a vacuum space of 15 Å in the non-periodic direction was adopted to avoid spurious interactions between the periodic images. The stability of the obtained structures were tested with phonon spectrum analysis using density functional perturbation theory (DFPT)[33] and high temperature *ab initio* molecular dynamic (MD) calculations considering a microcanonical ensemble[29].

A large variety of borophene polymorphs with vacancies have been reported and it has been shown that stability of these systems is mainly provided by vacancy patterns[7,11,34]. On the other hand, ideal borophene crystals without defects are scarce[10,35]. Motivated with the buckled structure of δ_6-borophene (belonging to Pmmn space group) where stability is enhanced by out-of-plane distortions[9,10] inDstead of vacancies, we seek for the possibility of obtaining ideal washboard structures of borophene which are not planar but have puckered geometries. Starting with various initial configurations and following structural optimizations without any constraint, we obtain a geometry similar to washboard structure as shown in Fig.1(a). However, different from the reported washboard structures of 2D Group VA systems, there is an additional atom at the center of hexagon (which can be noticed from the top view in Fig.1(a)) and accordingly, we label this structure (belonging to *Pbcm* space

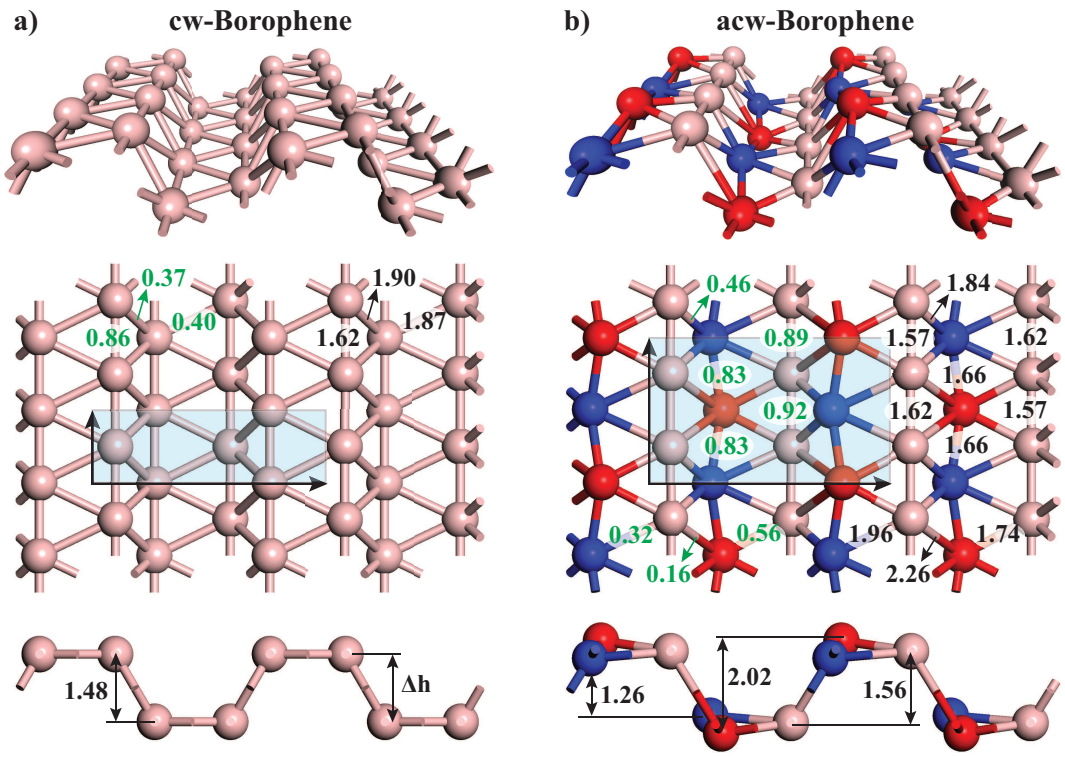

FIG. 1. Perspective, top, and side views of the optimized atomic structures of (a) centered-washboard (cw) and (b) asymmetric centered-washboard (acw) borophene, respectively. The unit cells are shown by shaded rectangles. Bond orders (green), puckering height (Δh) and bond lengths (black) are indicated. Blue and red spheres emphasize the distorted boron atoms.

group) as centered-washboard (cw) to denote the difference. The unit cell of symmetric cw-borophene is rectangular with lattice constants of 1.61 Å and 5.11 Å. The boron atoms form two different sublattices in this system at which atoms are puckered with a height (Δh) of 1.48 Å. Also, boron atoms located at the same sublattice maintain similar bond length pattern. Here every B atom has six neighbors with three distinct bonds having lengths of 1.62 Å, 1.87 Å, and 1.90 Å. Next, we compute the cohesive energy (per B atom), which is defined as: $E_c = (N * E[B] - E_T[\text{borophene}])/\text{N}$ where $E[B]$, $E_T[\text{borophene}]$, and N represent the energy of single B atom, the total energy of the optimized borophene structure, and the number of B atoms in the unit cell, respectively. E_c is calculated as 5.72 eV/atom which is slightly less than that is reported for synthesized buckled borophene (5.74 eV/atom)[10]. Despite its relatively high E_c, cw-borophene is found to be unstable due to imaginary phonon modes that appear in phonon dispersions. In phonon band structure the soft longitudinal acoustic modes emerges nearby the Γ point as shown in Fig.2(a). Eigenvectors, correspond-

ing to these negative phonon modes, can be used to refine the ionic positions of B atoms by shifting their positions along the softest mode which leads a distortion in this case. Additionally, MD simulations (which is performed for 12 × 4 super cell at 200 K, 400 K, 600 K, 800 K for in total 5 ps simulation time) indicate that the structure of cw-borophene is maintained up to 800 K but with distortions along vertical and horizontal directions starting from the temperatures as low as 200 K (Fig.2(c)).

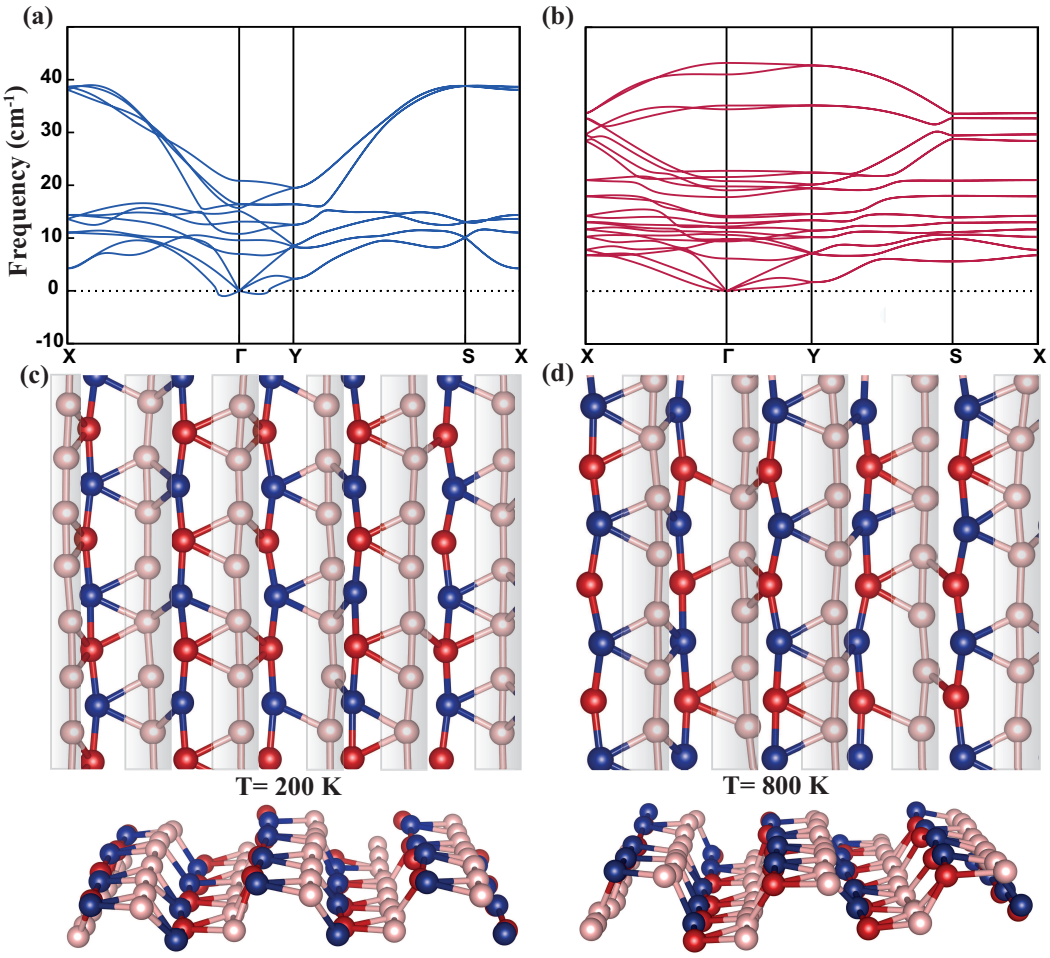

FIG. 2. The phonon spectrum of (a) cw- and (b) acw-borophene, and snapshots of molecular dynamics simulations of (c) cw-borophene at 200 K and (d) acw-borophene at 800 K.

The analysis of phonon spectrum and MD simulations lead us to a new polymorph, namely asymmetric centered-washboard (acw) borophene which is obtained with 2×1 super cell allowing the necessary reconstruction (Fig. 1(b)). The unit cell of acw-borophene is also rectangular with lattice constants of 3.19 Å and 5.3 Å. B atoms in acw-borophene have

significantly different bonding scheme than the symmetric geometry, where the bond lengths interchangeably differs even at the same sublattice (also quantified with bond order data) as shown in Fig. 1(b). Furthermore, there are two different Δh values, 1.26 Å and 2.02 Å depending on the position of B atom, indicating a varying hybridization of B atoms. acw-borophene has orthorhombic symmetry and belongs to $Pmn2_1$ space group different than other recently proposed $Pmmn$ and $8-Pmmn$ borophene systems[35,36]. E_c is calculated as 5.73 eV/atom which is lower than the bulk boron but within the range of other reported 2D boron polymorphs[9,34,37]. When compared E_c(acw) is slightly higher than ($\sim$10 meV/atom) E_c(cw)-borophene. The increase in E_c (or decrease in total energy) upon distortion signals the possibility of Peierls instability (see below). The optimized structure of acw-borophene has no negative frequencies in phonon spectrum and the system is thermodynamically stable even at high temperatures up to 800 K as presented in Fig. 2(d). These results confirm that acw-borophene is not a metastable configuration but corresponds to a stable, local minimum in Born-Oppenheimer energy surface. The structural parameters and crystallographic positions of the cw- and acw-borophene are reported as Supporting Information[38].

Revealing the structural properties and stability, we examine the electronic structures of the considered systems. The analysis of band structures of cw- and acw-borophene can elucidate the origin of the structural reconstruction. The band structure of cw-borophene is metallic with Dirac-like cones, mostly composed of p_z orbitals and contritions of each B atom are the same (Fig.3(a)). The cone along the X-G and Y-S line is 0.42 eV and 0.09 eV below E_F. The downward shift of the Dirac cones indicates excess of electrons in cw-borophene unlike to β_{12} sheet with vacancies.[15] Similar to buckled-borophene, electronic properties of cw-borophene is anisotropic and system is metallic along X-G and Y-S directions where Dirac cones are located. Interestingly, acw-borophene is a semiconductor with an indirect band gap of 0.39 eV along X-G direction as shown in Fig. 3(b). Bands crossings and splitting around the E_F are shown with green solid lines. Additionally, as shown in atomic-resolved partial density of states (PDOS), the attribution of distorted boron atoms to the band structure is not equivalent (Fig. 3(b)). Subsequent to the DFT-PBE results, the electronic band structures are calculated with hybrid functionals (HSE06)[32] to further confirm the obtained results. The resulting band structures with HSE06 have the same character, only the band gap increases to 0.69 eV[38]. This metal to semiconductor transition indicates that acw-borophene is stabilized with structural reconstruction due to Peierls distortion and band

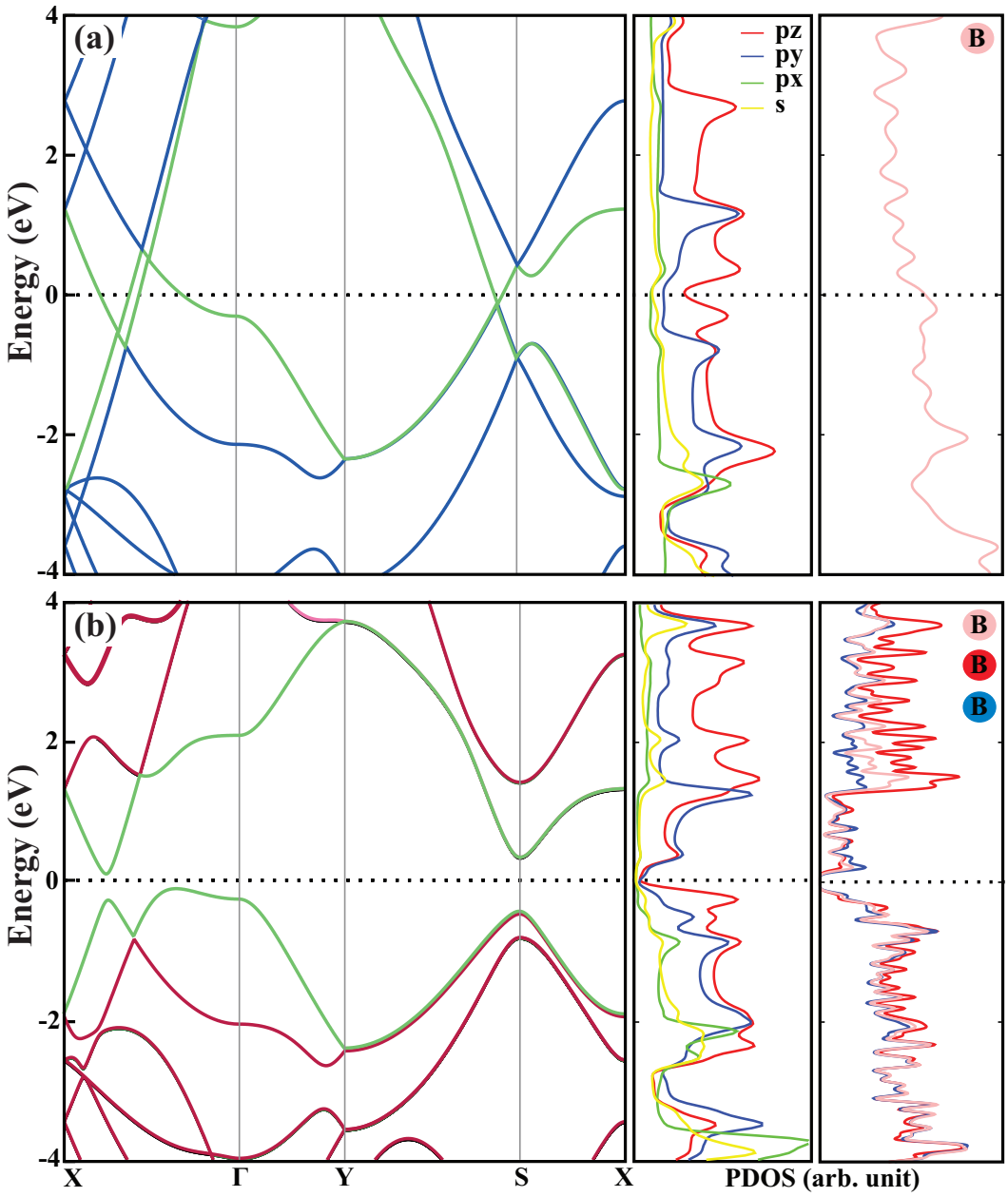

FIG. 3. Electronic structure of (a) cw- and (b) acw-borophene with orbital- and atomic-resolved partial density of states (PDOS). The bands which split upon distortion are shown with green solid lines. Fermi level (E_F) is set to zero and is shown by dotted lines.

gap opening reduces the total energy of the system. The Peierls instability for 1D metals are recently extended for 2D systems with the concept of charge density waves induced by nesting of Fermi surface[12,39,40]. It should be also noted that, acw-borophene is the only semiconductor polymorph of borophene reported so far with no vacancies/defects.

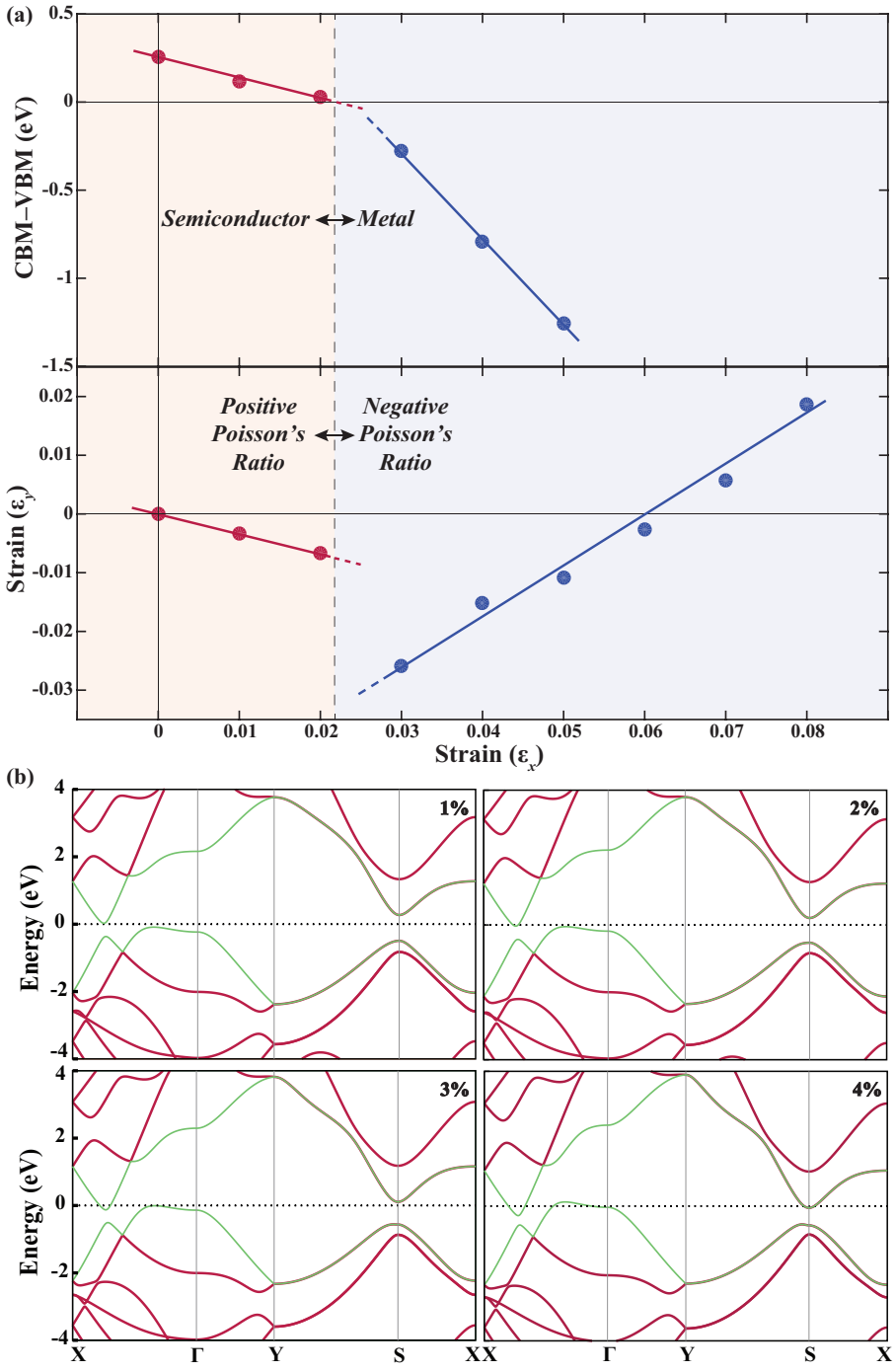

FIG. 4. (a) The variation of the electronic energy band gap and the equilibrium strain along y-direction (ϵ_y) with respect to applied strain along x direction (ϵ_x). The band gap values are extended to the metallic state by following the difference between the minimum of the conduction band (CBM) and the maximum of the valence band (VBM) after the transition. (b) the variations in the electronic band structure of acw-borophene upon applied uniaxial strain along ϵ_x.

Finally, we examine the effect of tensile strain on acw-borophene to mimic lattice-mismatched substrates and also it has been known that the properties of 2D materials can be tuned by strain engineering[41]. We investigate uniaxial strain up to %8, which covers low and high tensile strain levels. As shown in Fig. 4(a), the gap between conduction band minimum (CBM) and valence band maximum (VBM) gradually decreases with increasing strain and totally closes at ∼3%. Interestingly, at this strain level distortion in virtue of Peierls instability is removed and system transforms back into symmetric cw-borophene. This indicates that there is a trade off between structural deformation and energy gained due to band gap opening and once gap closes the structural phase transition accompanies electronic phase transition simultaneously. Moreover, Peierls instability not only affects the electronic properties of the system but also drastically changes the mechanical response. As shown in Fig.4(b), for acw-borophene, while strain increases along x-direction (ϵ_x), it tends to decrease along transverse-direction (ϵ_y) indicating positive Poisson's ratio (ν=-$\epsilon_y/\epsilon_x \approx$ 0.35). On the other hand, for $\epsilon_x \approx 0.03$ where the gap closes and distortion is altered, ϵ_y abruptly starts to increase with increasing ϵ_x making ν negative (-0.25). This suggests that cw-borophene which can be stabilized with strain, has an intrinsic auxetic behavior similar to phosphorene[42] and graphene with vacancies[43]. Negative ν values have been also reported for other metallic phases of borophene[10], but the magnitudes are much smaller compared to the one that is calculated for cw-borophene. The similar results are obtained when calculations are repeated with biaxial strain instead of uniaxial strain[38].

In conclusion, we predict a new, semiconducting, stable phase of borophene without defects, namely asymmetric centered-washboard (acw) structure which is formed by structural reconstructions due to Peierls instability in two-dimensions. The stability of aforementioned polymorph is provided in combination of the puckered geometry and Peierls distortion. The symmetric (cw) metallic system is sensitive to Peierls instability and acw-borophene becomes a semiconductor following structural transformation. Applying uniaxial or biaxial tensile strain to acw-borophene gradually lowers the band gap, and once it is fully closed, the system transforms back to the symmetric metallic state. Interestingly, transformation not only affects the electronic structure but also drastically modifies the mechanical response in parallel. While the system exhibits positive Poisson's ratio in semiconducting regime, Poisson's ratio abruptly becomes negative once system becomes metallic. The prediction of stable, semiconducting polymorph of borophene without defects and tunability of its elec-

tronic and mechanical response with strain can extend the usage of boron sheets in variety of nanoelectronic applications.

This work was supported by the Scientific and Technological Research Council of Turkey (TUBITAK) under Project No 115F088. The calculations were performed at TUBITAK ULAKBIM, High Performance and Grid Computing Center (TR-Grid e-Infrastructure) and the National Center for High Performance Computing of Turkey (UHeM) under grant no. 5003622015. E.D. acknowledges support from The Turkish Academy of Sciences - Outstanding Young Scientists Award Program (TUBA-GEBIP).

---

* durgun@unam.bilkent.edu.tr

[1] A. K. Singh, A. Sadrzadeh, and B. I. Yakobson, Nano Lett. **8**, 1314 (2008).

[2] H.-J. Zhai, Y.-F. Zhao, W.-L. Li, Q. Chen, H. Bai, H.-S. Hu, Z. A. Piazza, W.-J. Tian, H.-G. Lu, Y.-B. Wu, *et al.*, Nat. Chem. **6**, 727 (2014).

[3] Y. Yang, Z. Zhang, E. S. Penev, and B. I. Yakobson, Nanoscale **9**, 1805 (2017).

[4] W.-L. Li, T. Jian, X. Chen, T.-T. Chen, G. V. Lopez, J. Li, and L.-S. Wang, Angew. Chem. **128**, 7484 (2016).

[5] Z. A. Piazza, H.-S. Hu, W.-L. Li, Y.-F. Zhao, J. Li, and L.-S. Wang, Nat. Commun. **5**, 3113 (2014).

[6] W. Huang, A. P. Sergeeva, H.-J. Zhai, B. B. Averkiev, L.-S. Wang, and A. I. Boldyrev, Nat. Chem. **2**, 202 (2010).

[7] E. S. Penev, S. Bhowmick, A. Sadrzadeh, and B. I. Yakobson, Nano Lett. **12**, 2441 (2012).

[8] H. Tang and S. Ismail-Beigi, Phys. Rev. Lett. **99**, 115501 (2007).

[9] X.-F. Zhou, X. Dong, A. R. Oganov, Q. Zhu, Y. Tian, and H.-T. Wang, Phys. Rev. Lett. **112**, 085502 (2014).

[10] A. J. Mannix, X.-F. Zhou, B. Kiraly, J. D. Wood, D. Alducin, B. D. Myers, X. Liu, B. L. Fisher, U. Santiago, J. R. Guest, *et al.*, Science **350**, 1513 (2015).

[11] B. Feng, J. Zhang, Q. Zhong, W. Li, S. Li, H. Li, P. Cheng, S. Meng, L. Chen, and K. Wu, Nat. Chem. **8**, 563 (2016).

[12] X. Liu, Z. Zhang, L. Wang, B. I. Yakobson, and M. C. Hersam, Nat. Mater. (2018), 10.1038/s41563-018-0134-1.

[13] Z. Zhang, E. S. Penev, and B. I. Yakobson, Nat. Chem. **8**, 525 (2016).

[14] M. Gao, Q.-Z. Li, X.-W. Yan, and J. Wang, Phys. Rev. B **95**, 024505 (2017).

[15] B. Feng, O. Sugino, R.-Y. Liu, J. Zhang, R. Yukawa, M. Kawamura, T. Iimori, H. Kim, Y. Hasegawa, H. Li, *et al.*, Phys. Rev. Lett. **118**, 096401 (2017).

[16] B. Peng, H. Zhang, H. Shao, Y. Xu, R. Zhang, and H. Zhu, J. Mater. Chem. C **4**, 3592 (2016).

[17] B. Mortazavi, O. Rahaman, A. Dianat, and T. Rabczuk, Phys. Chem. Chem. Phys. **18**, 27405 (2016).

[18] H. Sun, Q. Li, and X. Wan, Phys. Chem. Chem. Phys. **18**, 14927 (2016).

[19] H. Xiao, W. Cao, T. Ouyang, S. Guo, C. He, and J. Zhong, Sci. Rep. **7**, 45986 (2017).

[20] A. Lherbier, A. R. Botello-Méndez, and J.-C. Charlier, 2D Mater. **3**, 045006 (2016).

[21] Z. Zhang, A. J. Mannix, Z. Hu, B. Kiraly, N. P. Guisinger, M. C. Hersam, and B. I. Yakobson, Nano Lett. **16**, 6622 (2016).

[22] L. Adamska, S. Sadasivam, J. J. Foley, P. Darancet, and S. Sharifzadeh, J. Phys. Chem. C **122**, 4037 (2018).

[23] Y. Chen, G. Yu, W. Chen, Y. Liu, G.-D. Li, P. Zhu, Q. Tao, Q. Li, J. Liu, X. Shen, H. Li, X. Huang, D. Wang, T. Asefa, and X. Zou, J. Am. Chem. Soc. **139**, 12370 (2017).

[24] H. Zhou, Y. Cai, G. Zhang, and Y.-W. Zhang, NPJ 2D Mater. Appl. **1**, 14 (2017).

[25] X. Liu, Z. Wei, I. Balla, A. J. Mannix, N. P. Guisinger, E. Luijten, and M. C. Hersam, Sci. Adv. **3** (2017).

[26] Z. Zhang, E. S. Penev, and B. I. Yakobson, Nat. Chem. **8**, 525 (2016).

[27] W. Kohn and L. J. Sham, Phys. Rev. **140**, A1133 (1965).

[28] P. Hohenberg and W. Kohn, Phys. Rev. **136**, B864 (1964).

[29] G. Kresse and J. Furthmüller, Phys. Rev. B **54**, 11169 (1996).

[30] P. E. Blöchl, Phys. Rev. B **50**, 17953 (1994).

[31] J. P. Perdew, K. Burke, and M. Ernzerhof, Phys. Rev. Lett. **77**, 3865 (1996).

[32] J. Heyd, G. E. Scuseria, and M. Ernzerhof, J. Chem. Phys. **118**, 8207 (2003).

[33] A. Togo and I. Tanaka, Scr. Mater. **108**, 1 (2015).

[34] X. Wu, J. Dai, Y. Zhao, Z. Zhuo, J. Yang, and X. C. Zeng, ACS Nano **6**, 7443 (2012).

[35] A. Lopez-Bezanilla and P. B. Littlewood, Phys. Rev. B **93**, 241405 (2016).

[36] X.-F. Zhou, X. Dong, A. R. Oganov, Q. Zhu, Y. Tian, and H.-T. Wang, Phys. Rev. Lett. **112**, 085502 (2014).

[37] F. Ma, Y. Jiao, G. Gao, Y. Gu, A. Bilic, Z. Chen, and A. Du, Nano Letters **16**, 3022 (2016).

[38] See Supplemental Material for the cell parameters and atomic positions of cw- and acw-borophene; electronic band structures obtained with HSE06 under uniaxial strain; and electronic band structures under biaxial strain.

[39] S. Borisenko, A. Kordyuk, A. Yaresko, V. Zabolotnyy, D. Inosov, R. Schuster, B. Büchner, R. Weber, R. Follath, L. Patthey, *et al.*, Phys. Rev. Lett. **100**, 196402 (2008).

[40] M. Johannes and I. Mazin, Phys. Rev. B **77**, 165135 (2008).

[41] S. Cahangirov, H. Sahin, G. Le Lay, and A. Rubio, "Strain engineering of 2d materials," in *Introduction to the Physics of Silicene and other 2D Materials* (Springer International Publishing, Cham, 2017) pp. 87–96.

[42] H. Wang, X. Li, P. Li, and J. Yang, Nanoscale **9**, 850 (2017).

[43] J. N. Grima, S. Winczewski, L. Mizzi, M. C. Grech, R. Cauchi, R. Gatt, D. Attard, K. W. Wojciechowski, and J. Rybicki, Adv. Mater. **27**, 1455 (2015).